Available online at www.sciencedirect.com
ScienceDirect
Journal of Colloid and Interface Science 311 (2007) 469–474
JOURNAL OF Colloid and Interface Science
www.elsevier.com/locate/jcis

Preparation of magnetite nanocrystals with surface reactive moieties by one-pot reaction

Fengqin Hu, Zhen Li, Chifeng Tu, Mingyuan Gao *

Key Laboratory of Colloid, Interface Science and Chemical Thermodynamics, Institute of Chemistry, Chinese Academy of Sciences, Zhong Guan Cun, Bei Yi Jie 2, Beijing 100080, China

Received 25 January 2007; accepted 13 March 2007

Available online 20 March 2007

Abstract

By one-pot reaction, biocompatible magnetite nanocrystals with surface reactive moieties were prepared through the thermal decomposition of $Fe(acac)_3$ in 2-pyrrolidone using α,ω-dicarboxyl-terminated poly(ethylene glycol) as surface capping molecule. The successful conjugation between the magnetite nanocrystals and 9-amino acridine on the one hand demonstrates the existence of free carboxylic groups from PEG binding on the particle surface, on the other hand may also lead to a new type of magneto-optical materials as well as magneto-drugs.

Keywords: Reactive surface moieties; Biocompatible Fe_3O_4 nanocrystals; One-pot reaction

1. Introduction

The surface properties of magnetic nanocrystals are very important not only because they have great influence on the magnetic properties [1], but also because they strongly determine the solubility (or dispersibility) of the magnetic nanocrystals in various chemical media and further lead to different environmental compatibilities for the nanocrystals [2]. More importantly, different types of surface reactive moieties also provide versatile choices for coupling magnetic nanocrystals with various biomaterials in applications such as biodetection and bioseparation [3], target-drug delivery [4], magnetic resonance imaging (MRI) [5–7], and hyperthermia treatment of cancers [8], and etc. For some of these applications, an effective coupling between the magnetic nanocrystals and some bioligands is often required for enhancing the interactions between nanocrystals and receptors via the specific ligand–receptor interactions. For examples, Gu and coworkers firstly prepared FePt nanocrystals and then obtained amino groups stemming from the particle surface upon modification. The FePt-vancomycin conjugates formed subsequently via the amino groups presented great binding ability for capturing Gram-positive bacteria at ultralow concentrations [3a]. Similarly, Weissleder's group adopted *N*-succinimidyl-3-(2-pyridyldithio) propionate as a linker to couple a fluorescent-labeling short HIV-Tat peptide with iron oxide nanoparticles via the amino residues on the particle surface. The resultant conjugates were able to efficiently internalize into the progenitor cells through the HIV-Tat, which made the conjugates useful for tracking the differentiation and fate of cells in vivo by MRI, fluorescence imaging and radioscopy [6].

Although these results are very exciting and promising for exploring new applications for the superparamagnetic nanocrystals, so far there remains no simple way for producing magnetic particles with surface reactive moieties. In the aforementioned examples, sophisticated post-preparative modifications were required no matter the magnetic nanoparticles were prepared by thermal decomposition method [3,5] or coprecipitation method [6]. For most samples obtained by the thermal decomposition method, multifunctional ligands are necessarily required as both phase transfer agents, to transfer the nanocrystals from organic phase to water, and surface coupling agents to provide the particles with surface reactive moieties for further linking bioligands [5]. For magnetic nanoparticles obtained by (co)precipitation method, surface modification by polymer is often adopted. However, some high-molecular weight poly-

* Corresponding author. Fax: +86 10 82613214.
E-mail address: gaomy@iccas.ac.cn (M.Y. Gao).

0021-9797/$ – see front matter
doi:10.1016/j.jcis.2007.03.023

mer can cause unwanted side effects at high dose level with respect to in vivo applications [9]. Therefore, it is necessary to develop a facile approach for preparing biocompatible magnetic nanocrystals with surface reactive moieties.

Previously, we have demonstrated that water-soluble magnetic nanocrystals can directly be prepared by pyrolyzing ferric acetylacetonate ($Fe(acac)_3$) or boiling ferric chloride hydrate in 2-pyrrolidone [10,11]. In a similar way, biocompatible Fe_3O_4 nanocrystals could also be prepared in the presence of monocarboxyl-terminated poly(ethylene glycol) (MPEG–COOH) by covalently binding MPEG–COOH to the particle surface via carboxylic group. The in vivo experiments revealed that the MPEG-modified Fe_3O_4 nanocrystals presented a satisfying blood circulation time due to their reduced nonspecific targeting (plasma protein adsorption) [12]. Following on from this one-pot reaction approach, recently we further developed the synthetic approach for preparing biocompatible magnetite nanocrystals with surface reactive moieties. In this paper, we report the details for preparing Fe_3O_4 nanocrystals capped by α,ω-dicarboxyl-terminated PEG (denoted by Fe_3O_4@PEG–COOH). A conjugation reaction between the resultant Fe_3O_4 nanocrystals and 9-amino acridine was performed to demonstrate the existence of free carboxylic groups from the PEG molecules binding on the particle surface.

2. Experimental

9-Amino acridine chloride (9-AA·HCl, TCI, A0619), 1-ethyl-3-(3-dimethylaminopropryl) carbodiimide hydrochloride (EDC·HCl, Pierce, 22980), *N*-hydroxysulfosuccimimide sodium salt (Sulfo-NHS, Fluka, 56485) and ferric acetylacetonate ($Fe(acac)_3$, Aldrich, 51700-3) were used as received. 9-AA was obtained by dropping ammonia solution (25%) into an aqueous solution of 9-AA·HCl. The precipitate obtained was collected by centrifugation followed by washing with double-distilled water for several cycles. Three samples of α,ω-dicarboxyl-terminated PEG (HOOC–PEG–COOH) with different molecular weight ($M_n = 2000, 4000$ and 6000) were prepared by a method described in literature [12].

The preparations of Fe_3O_4@PEG–COOH were conducted in a quite similar way as previously reported [10–12]. Typically, the 12 nm magnetite nanocrystals were prepared as follows: 0.9 mmol $Fe(acac)_3$ and 1.1 mmol HOOC–PEG–COOH ($M_n = 2000$) were dissolved in 90 mL 2-pyrrolidone. The resultant mixture was purged with nitrogen for 30 min to remove oxygen and then boiled for 70 min at 240 °C. After that, the reaction mixture was cooled to room temperature followed by addition of a mixture of acetone and ether. Consequently, a black and sticky precipitate was obtained. The precipitate was subsequently re-dissolved in double-distilled water and then subjected to a 2-day dialysis to remove species with molecular weight smaller than 12000. Afterwards, the nanocrystals were sedimentated from the aqueous solution by the mixture of acetone and ether, and collected with the aid of a permanent magnet (0.5 T). The 27 nm magnetite nanocrystals were prepared similarly. In detail, 20 mL purified 2-pyrrolidone solution containing 2.0 mmol $Fe(acac)_3$ and 1.5 mmol HOOC–PEG–COOH ($M_n = 4000$) was prepared and purged with nitrogen for 30 min to remove oxygen. Then it was subjected to a reflux of 10 h. After that, the reaction mixture was treated the same way as that for the 12 nm sample.

9-AA was covalently bonded to the surface of the magnetite nanocrystals via an EDC-mediated amydation reaction. Typically, 4.8 mg EDC·HCl and 10.0 mg sulfo-NHS were added into 15 mL aqueous solution of purified magnetite nanocrystals (1 mg mL^{-1} Fe_3O_4). After approximately 10 min, 0.5 mL acetone solution containing 1.5 mg 9-AA was introduced followed by adjusting the pH of the reaction system to 7.5 using 1 M NaOH. The reaction was usually allowed for 4 h and then the acetone/ether mixture was added to precipitate the conjugates. After being washed with acetone for several times until no fluorescence was detected from the supernatant, the resultant conjugates were re-dispersed into water for further spectroscopy measurements.

Both the mother magnetite nanocrystals and resultant conjugates were characterized by TEM (Transmission Electron Microscopy), XRD (X-ray Diffraction), FTIR (Fourier Transform Infrared Spectroscopy), VSM (Vibrating Sample Magnetometer), elemental analysis, UV–vis absorption, and excitation and fluorescence spectroscopy. TEM images were obtained on a JEM-100CX II electron microscope operating at an acceleration voltage of 100 kV. XRD patterns were obtained with a Regaku D/Max-2500 diffractometer equipped with a rotating anode and a Cu$K_{\alpha 1}$ radiation source ($\lambda = 1.54056$ Å). FTIR spectra were performed on a Bruker EQUINOX55 Fourier transform infrared spectrometer. Room temperature magnetization was measured on a homemade vibrating sample magnetometer. UV–vis absorption spectra, fluorescent spectra were recorded at room temperature with a Cary 50 UV–vis spectrophotometer and a Cary Eclipse fluorescence spectrophotometer, respectively.

3. Results and discussion

Fig. 1a shows a representative TEM image of Fe_3O_4 nanocrystals whose average particle size is 12.2 nm with a standard deviation (s.d.) of 1.8 nm. The crystalline structure was identified by powder X-ray diffraction (XRD) as shown in Fig. 2. The positions and relative intensities of all diffraction peaks match well with those from the JDPCS card (19-0629) for magnetite. The average particle size of 12.6 nm, calculated by Scherrer's formula according the XRD pattern, is in very good agreement with that determined by TEM, suggesting that the Fe_3O_4 nanoparticles possess a single crystal structure.

In fact, in comparison with the particles smaller than 20 nm, there are fewer reports on magnetic Fe_3O_4 particles of 20–50 nm which still exhibit satisfying water-dispersibility and biocompatibility. It was demonstrated that through the current synthetic route, by varying the following parameters such as the concentration of $Fe(acac)_3$, reaction time, molar ratio between HOOC–PEG–COOH and $Fe(acac)_3$, as well as molecular weight of HOOC–PEG–COOH, the particle size can effectively be tuned. Fig. 1b is a typical image of larger magnetite nanocrystals obtained by refluxing 20 mL 2-pyrrolidone

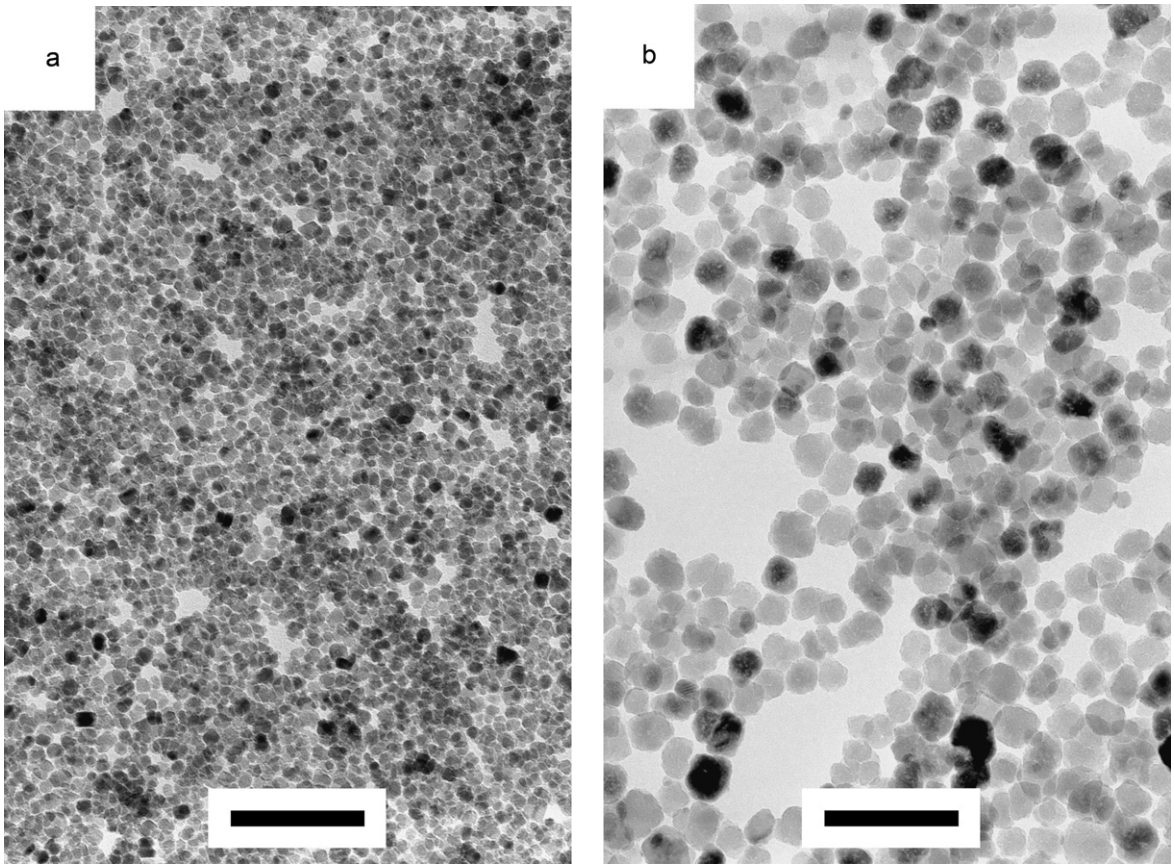

Fig. 1. TEM images of 12 and 27 nm magnetite nanocrystals. The initial concentrations of $Fe(acac)_3$ for the preparations of these two samples were 0.01 and 0.1 M, respectively. The scale bar corresponds to 100 nm.

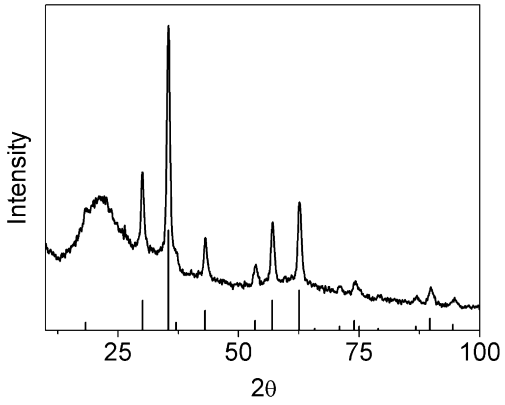

Fig. 2. Powder X-ray diffractograms of 12 nm magnetite nanoparticles. Bottom: JCPDS card (19-0629) data for magnetite.

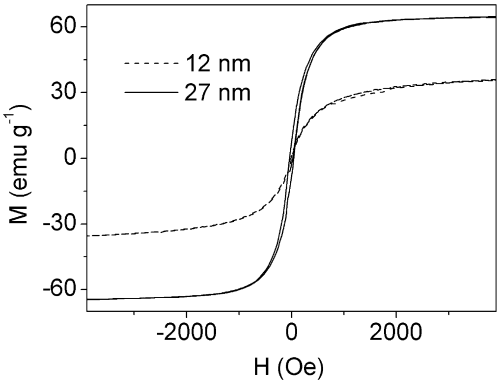

Fig. 3. Room-temperature magnetization curves of 12 (- - -) and 27 nm (—) magnetite nanocrystals.

solution containing 2.0 mmol $Fe(acac)_3$ and 1.5 mmol HOOC–PEG–COOH ($M_n = 4000$) for 10 h. The average particle size of this sample is 27.0 ± 4.1 (±s.d.) nm. The room-temperature magnetization curves shown in Fig. 3 demonstrate that 12 nm Fe_3O_4 nanoparticles are superparamagnetic, while 27 nm particles are ferrimagnetic with a remanent magnetization of about 7 emu g^{-1}. The saturation magnetizations of these two samples determined by vibrating sample magnetometer are 35 and 64 emu g^{-1}, respectively.

Two questions may be raised for covalently binding α,ω-dicarboxyl-terminated PEG to the surface of Fe_3O_4 nanocrystals in comparison with monocarboxyl-terminated PEG: (1) whether HOOC–PEG–COOH acts as a linker between particles; and (2) whether the two carboxylic groups from one HOOC–PEG–COOH molecule fold back and simultaneously bind on the surface of the same Fe_3O_4 particle.

To answer the first question more preparations were performed by varied synthetic parameters. It was found out that when the initial concentration of the $Fe(acac)_3$ was increased from 0.01 to 0.05 M, the thermal decomposition reactions led to dimers, trimers or even larger aggregates of nanoparticles 40 min after reflux in the presence of equal mol of HOOC–

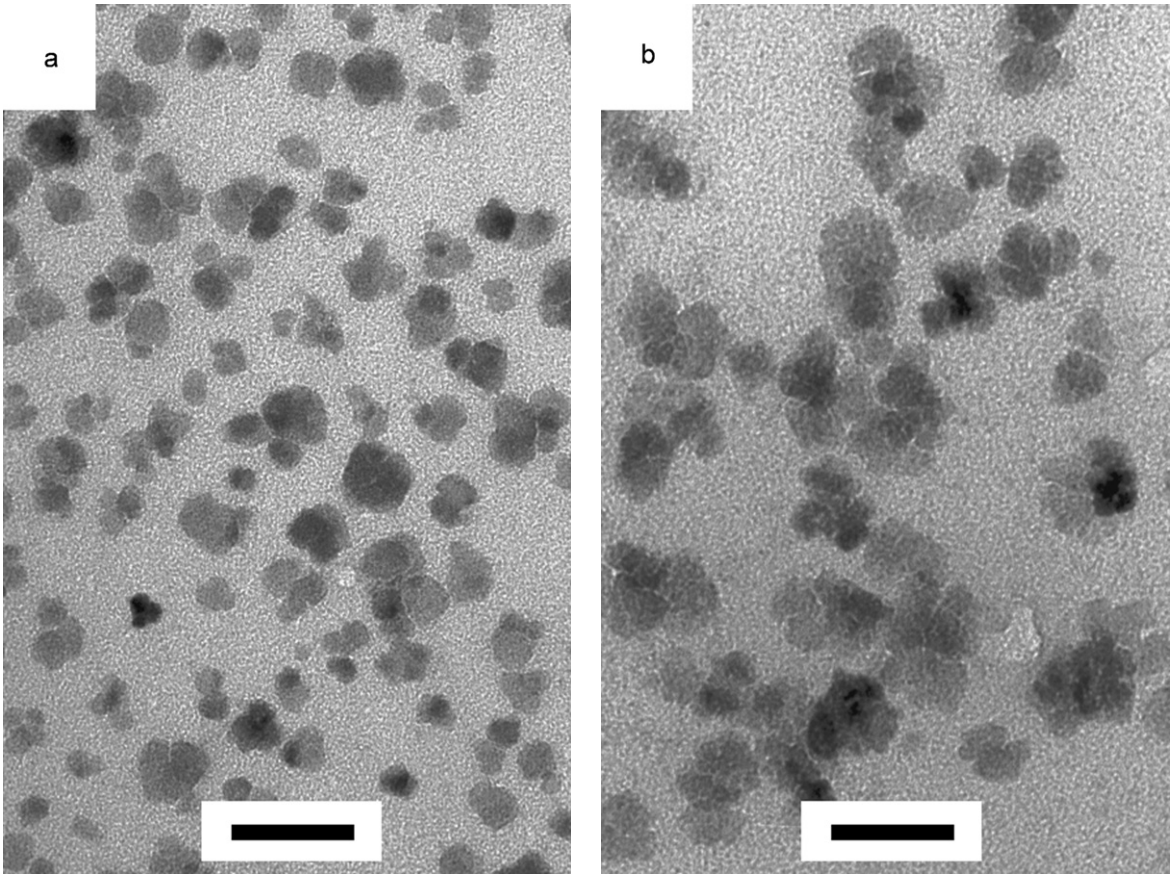

Fig. 4. TEM images of magnetite nanocrystals prepared with the initial concentrations of $Fe(acac)_3$ being of 0.05 M in the presence of equal mol of HOOC–PEG–COOH of $M_n = 6000$ (a) and 1.5 fold mol of HOOC–PEG–COOH of $M_n = 4000$ (b). The scale bar corresponds to 40 nm.

PEG–COOH ($M_n = 6000$) (Fig. 4a) or 1.5 fold mol of HOOC–PEG–COOH ($M_n = 4000$) (Fig. 4b), which strongly suggests that HOOC–PEG–COOH can bridge different particles to form aggregates when the initial concentrations of the reactants were high enough. In comparison with the particles shown in Fig. 4b, further increasing the initial concentration (0.1 M) of the reactants favors the formation of larger crystals (Fig. 1b) instead of the dimmers and trimers, implying that the 27 nm nanocrystals are probably formed by merging nanocrystals in small aggregates upon prolonged reflux since the average size of clearly identifiable small aggregates is about 30.7 ± 3.6 (s.d.) nm. Nonetheless, similar small aggregates with clear sharp edge between neighboring particles were not present in the samples shown in Fig. 1 with a lower particle density on the TEM copper grids. Moreover, the aqueous dispersions of the 12 and 27 nm Fe_3O_4 particle samples presented quite good stability. Therefore, it can be concluded that under proper preparative conditions, aggregation caused by the coupling effect of HOOC–PEG–COOH can be avoided.

Comparing with the first question, the second question is more difficult to answer. Although the very good aqueous dispersibility of the 12 and 27 nm samples in pure water supports that HOOC–PEG–COOH is covalently attached to the particle surface, the question on the availability of free carboxylic groups on the particle surface remains open. Due to the limited number of the carboxylic groups in the whole organic content in the particle samples, it is difficult to detect the free carboxylic groups by conventional spectroscopy. Therefore, 9-amino acridine (9-AA), as a fluorescent probe, was coupled with the magnetic nanocrystals via an EDC [1-ethyl-3-(3-dimethylaminopropyl) carbodiimide]-mediated reaction. Moreover, 9-AA is also an antibacterial, mutagenic, and antitumoral drug [13]. The successful coupling between 9-AA and magnetite nanocrystals could consequently lead to a novel type of magneto-optical materials as well as a new type of magneto-drugs which have been demonstrated to be very useful in many bioapplications [14].

The IR spectra of the 27 nm magnetite nanocrystals, 9-AA together with their corresponding conjugates are shown in Fig. 5. There are a number of observable differences among these three spectra. Firstly, four characteristic absorption bands of 9-AA appear in the spectrum of the conjugates, centered at 1662, 1637, 1594 and 1240 cm^{-1}, respectively. Secondly, the intensity ratio between peaks at 1637 and 1662 cm^{-1} is reversed in conjugates comparing with that in 9-AA. Thirdly, the characteristic absorption bands of PEG and Fe_3O_4 simultaneously appear in the spectrum of conjugates. They are the C–H asymmetric band at 2923 cm^{-1}, the C–H symmetric stretching band at 2864 cm^{-1}, the C–O–C stretching band at 1107 cm^{-1} from PEG [15], and the lattice absorption band at 585 cm^{-1} from magnetite nanocrystals [16]. Lastly, the conjugates present a very broad absorption band in the spectral region higher than 3000 cm^{-1}, which may possibly be attributed to the overlap

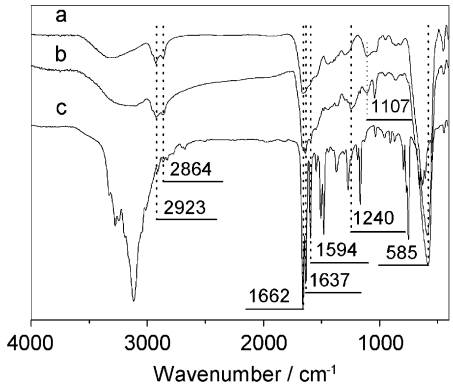

Fig. 5. FTIR spectra of the 27-nm magnetite nanocrystals (a), the Fe_3O_4–(9-AA) conjugates (b), and 9-AA (c).

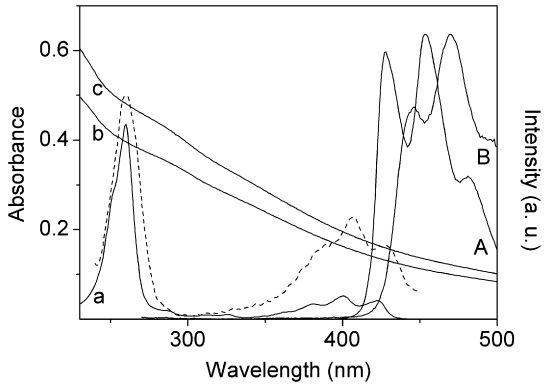

Fig. 6. UV–vis absorption spectra of 9-AA (a), 27-nm magnetite nanocrystals (b), and the conjugates of magnetite nanocrystals and 9-AA (c), together with the fluorescence spectra of 9-AA (A), the conjugates (B) and an excitation spectrum (- - -) of the conjugates monitored at 470 nm.

of the N–H stretching band at around 3115 cm^{-1} from 9-AA and the N–H stretching band at 3324 cm^{-1} from 2-pyrrolidone binding on the surface of magnetite nanocrystals. Since the conjugates were thoroughly washed with acetone for several cycles until no fluorescence was detected from the supernatant, the IR results suggest that 9-AA has successfully been coupled to the magnetite particle surface through the coupling reaction.

The conjugates were further characterized by conventional electron spectroscopy. The absorption, excitation and fluorescence spectra of 9-AA, magnetite nanocrystals, together with their conjugates are presented in Fig. 6. The absorbance of 9-AA is roughly superimposed on that of the magnetic nanocrystals leading to an enhanced absorbance for the conjugates. However, the photoluminescence of the conjugates turns out to be different from that of 9-AA. According to literature, the emission bands at 428 and 454 nm present in the fluorescence spectrum of pure 9-AA originate from 9-AA monomer, while the emission at 480 nm comes from the 9-AA dimers [17]. In the fluorescence spectrum of the conjugates, these bands shift to 440, 470 and 500 nm, respectively. In addition, the band intensity ratio between 440 and 470 nm is also larger than that for pure 9-AA. Nonetheless, the excitation spectrum of the conjugates monitored at 470 nm very much resembles the absorption spectrum of 9-AA, indicating that the fluorescence of conjugates does come from 9-AA covalently binding on the particle surface. Although the red-shifts in the fluorescence of the conjugates are not fully understood yet, at least they support that 9-AA is not simply adsorbed on the surface of the magnetic nanocrystals since no such red-shifts were observed from the control sample that was obtained by mixing 9-AA with the magnetite nanocrystals in the absences of both EDC·HCl and sulfo-NHS.

Table 1
Elemental analysis of the 12 nm Fe_3O_4 particle samples prior to and after the conjugation reaction

	W (wt%)	
	Fe_3O_4 nanocrystal	Fe_3O_4–9-AA conjugate
Nitrogen	2.4	2.6
Carbon	33.8	22.1

The conjugates were more quantitatively analyzed by elemental analysis by determining the weight percentages of both carbon and nitrogen elements in the 12 nm Fe_3O_4 particle samples prior to and after the conjugation reaction, the results are provided in Table 1. Prior to conjugation, the molar ratio of 2-pyrrolidone to HOOC–PEG–COOH was calculated to be around 7. Since the carbon weight percentage dropped drastically from 33.8 to 22.1 after the conjugation reaction, it can be deduced that some of HOOC–PEG–COOH molecules were disassociated with the particles during the conjugation reaction. TGA (Thermal Gravity Analysis) results further demonstrated that within the temperature range for the pyrolysis of PEG, the conjugates and the mother particles lost weight percentages of 9 and 19%, respectively, and this discrepancy supports that some of the PEG molecules left the particle surface during the conjugation reaction. Based on all these results as well as the variation of the weight percentage of nitrogen, the molar ratio between 9-AA and HOOC–PEG–COOH in the conjugate was estimated to be 0.56. Furthermore, the total number of the surface capping molecules including both PEG and 2-pyrrolidone on each 12 nm Fe_3O_4 particle was calculated to be around 1780 based on following assumptions: (1) Fe_3O_4 nanocrystals are in spherical form; (2) Fe_3O_4 nanocrystals have the same density as their corresponding bulk, i.e., 5.2 g cm^{-3}; and (3) the number of the surface capping molecules is identical to the number of Fe_3O_4 structural units on the particle surface. Then, the numbers of HOOC–PEG–COOH and 9-AA molecules on each (9-AA)-conjugated Fe_3O_4 particle was estimated to be around 110 and 60, respectively.

4. Conclusions

In summary, by one-pot reaction, through the thermal decomposition of $Fe(acac)_3$ in 2-pyrrolidone, biocompatible magnetite nanocrystals with surface reactive moieties were prepared using α,ω-dicarboxyl-terminated poly (ethylene glycol) as surface capping agent. The particle size was successfully tuned by varying the synthetic parameters. Experimental results imply that HOOC–PEG–COOH is covalently modified on the surface of Fe_3O_4 particles via at least one of its carboxylic

groups, leaving the second carboxylic group available for further chemical reaction. The availability of surface carboxylic moieties was indirectly demonstrated by its reaction with 9-AA. In addition, the successful coupling between the HOOC–PEG–COOH-coated Fe_3O_4 and 9-AA could also lead to a new type of magneto-optical materials as well as magneto-drugs.

Acknowledgments

Funding was provided jointly by an 863 project (2002AA-302201) and NSFC projects (20225313, 90206024).

References

[1] C.R. Vestal, Z.J. Zhang, J. Am. Chem. Soc. 125 (2003) 9828.
[2] M. Kim, Y. Chen, Y. Li, X. Peng, Adv. Mater. 17 (2005) 1429.
[3] (a) H. Gu, P.L. Ho, K.W.T. Tsang, L. Wang, B. Xu, J. Am. Chem. Soc. 125 (2003) 15702;
(b) C. Xu, K. Xu, H. Gu, X. Zhong, Z. Guo, R. Zheng, X. Zhang, B. Xu, J. Am. Chem. Soc. 126 (2004) 3392.
[4] S.J. Son, J. Reichel, B. He, M. Schuchman, S.B. Lee, J. Am. Chem. Soc. 127 (2005) 7316.
[5] Y.M. Huh, Y.W. Jun, H.T. Song, S. Kim, J.S. Choi, J.H. Lee, S. Yoon, K.S. Kim, J.S. Shin, J.S. Suh, J. Cheon, J. Am. Chem. Soc. 127 (2005) 12387.
[6] M. Lewin, N. Carlesso, C.H. Tung, X.W. Tang, D. Cory, D.T. Scadden, R. Weissleder, Nat. Biotechnol. 18 (2000) 410.
[7] F. Hu, L. Wei, Z. Zhou, Y. Ran, Z. Li, M.Y. Gao, Adv. Mater. 18 (2006) 2553.
[8] M. Johannsen, B. Thiesen, A. Jordan, K. Taymoorian, U. Gneveckow, N. Waldöfner, R. Scholz, M. Koch, M. Lein, K. Jung, S.A. Loening, Prostate 64 (2005) 283.
[9] A.S. Arbab, G.T. Yocum, W.L. Bashaw, A. Parwana, E.K. Jordan, H. Kalish, J.A. Frank, Mol. Imaging 3 (2004) 24.
[10] Z. Li, H. Chen, H. Bao, M.Y. Gao, Chem. Mater. 16 (2004) 1391.
[11] Z. Li, Q. Sun, M.Y. Gao, Angew. Chem. Int. Ed. 44 (2005) 123.
[12] Z. Li, L. Wei, M.Y. Gao, H. Lei, Adv. Mater. 17 (2005) 1001.
[13] A. Murza, S. Sánchez-Cortés, J.V. García-Ramos, Biospectroscopy 4 (1998) 327.
[14] (a) X. Montet, R. Weissleder, L. Josephson, Bioconjugate Chem. 17 (2006) 905;
(b) O. Veiseh, C. Sun, J. Gunn, N. Kohler, P. Gabikian, D. Lee, N. Bhattarai, R. Ellenbogen, R. Sze, A. Hallahan, J. Olson, M. Zhang, Nano Lett. 5 (2005) 1003;
(c) N. Kohler, C. Sun, A. Fichtenholtz, J. Gunn, C. Fang, M. Zhang, Small 2 (2006) 785.
[15] S. Herrwerth, T. Rosendahl, C. Feng, J. Fick, W. Eck, M. Himmelhaus, R. Dahint, M. Grunze, Langmuir 19 (2003) 1880.
[16] U. Schwertmann, R.M. Cornell, in: U. Schwertmann, R.M. Cornell (Eds.), Iron Oxides in the Laboratory—Preparation and Characterization, second ed., Wiley–VCH, Weinheim, 2000, chap. 1.
[17] P. Gangola, N.B. Joshi, D.D. Pant, Chem. Phys. Lett. 80 (1981) 418.